Dynamic Response of Wind Turbines to Theoretical 3D Seismic Motions Taking into Account the Rotational Component

L. Hermanns, M.A. Santoyo, L. E. Quirós, J. Vega, J. M. Gaspar-Escribano and B. Benito

***Abstract*—**We study the dynamic response of a wind turbine structure subjected to theoretical seismic motions, taking into account the rotational component of ground shaking. Models are generated for a shallow moderate crustal earthquake in the Madrid Region (Spain). Synthetic translational and rotational time histories are computed using the Discrete Wavenumber Method, assuming a point source and a horizontal layered earth structure. These are used to analyze the dynamic response of a wind turbine, represented by a simple finite element model. Von Mises stress values at different heights of the tower are used to study the dynamical structural response to a set of synthetic ground motion time histories

***Keywords*—**Synthetic seismograms, rotations, wind turbine, dynamic structural response

I. INTRODUCTION

ROTATIONAL ground motion analysis is a novel discipline of seismology that still presents significant unexplored fields. Accordingly, the development of instruments for recording rotational motions is limited. Thus, strong motion networks do not routinely measure these parameters. In this paper we compute a set of complete synthetic ground motion time histories (i. e., including both translational and rotational components) in order to evaluate the seismic response of a wind turbine. This structure is interesting because it presents a large inertial mass at the top and a rotating component around a horizontal axis. Different methods to calculate the dynamic response of the structure are examined. At this stage of the analysis, an unsophisticated finite element model seems a good choice for performing dynamical calculations. The structural response of the wind turbine is characterized by the maximum value of Von Mises stress at different levels of the tower. The target turbine site corresponds to a hypothetic site located at Madrid Region (Spain), where moderate events could take place. Values of the corresponding seismological parameters are selected accordingly. However, the upper soil layer of the Earth velocity model is very stiff. This should always be remembered when interpreting the results.

L. H., L.E.Q., J. V., J.M.G.-E. and B. B. are with Universidad Politécnica de Madrid, Spain (phone: +34913366441; e-mail: lutz.hermanns@upm.es; jorge.gaspar@upm.es).

M.A.S. is with Universidad Complutense de Madrid, Spain

II.. SYNTHETIC GROUND MOTIONS

The seismic inputs used in this work (translational and rotational time histories) were theoretically generated for an earth layered structure embedding a double couple point source at shallow depths. Seismic events were characterized by a specific focal mechanism, moment magnitude and a Source-time Function (SF) equivalent to an earthquake with circular finite rupture. The synthetic seismograms (accelerograms) were computed using the discrete wave-number method described by Bouchon and Aki (1977) [2] and Bouchon (1979) [1] for point dislocations. The earth wave velocity model assumed corresponds to the crustal properties of the south-eastern region of the Madrid Region, Spain (Corchete and Chourak, 2011) [3].

The set of synthetic seismograms used were generated for 30 different focal mechanisms and SF, located 23 km northeast of the wind turbine site. We assumed a Mw=5.5 earthquake at 6.0 km depth, which is the mean depth of seismicity in this region. The set of SF were randomly generated taking into account the mean properties of shallow crustal earthquakes of these magnitudes (Houston, 2007)[4]. SF were constructed assuming a lognormal shape with skewness $0.15<S_k<0.35$ (Houston, 2007) [4]. added with 20% of white noise, low pass filtered at a fc=25 Hz. Fig. 1 shows an example of two of the SF used in the study.

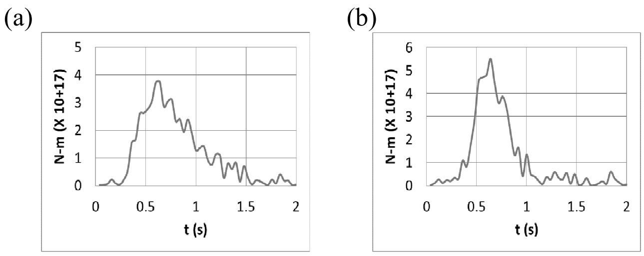

Fig. 1 Source Time Functions for two of the simulated earthquakes

Seismograms were synthesized up to a frequency of 75.0 Hz and low pass filtered with a 4 pole Butterworth filter with a cutoff frequency of 40 Hz. In this way, the highest usable frequency is about 35.0 Hz. Focal mechanism were also randomly generated taking into account the tectonic setting of the region. Once seismograms were generated, we obtained the time histories of rotations and angular accelerations by a finite difference modelization of the displacement gradient tensor. In

Fig. 2 we show an example of the synthetic accelerations and rotations used.

The results indicate that the frequency content of the modeled translational and rotational ground motions have large variations depending on the SF and focal mechanism assumed. Due to this, the response of the turbine structure could change depending on these conditions.

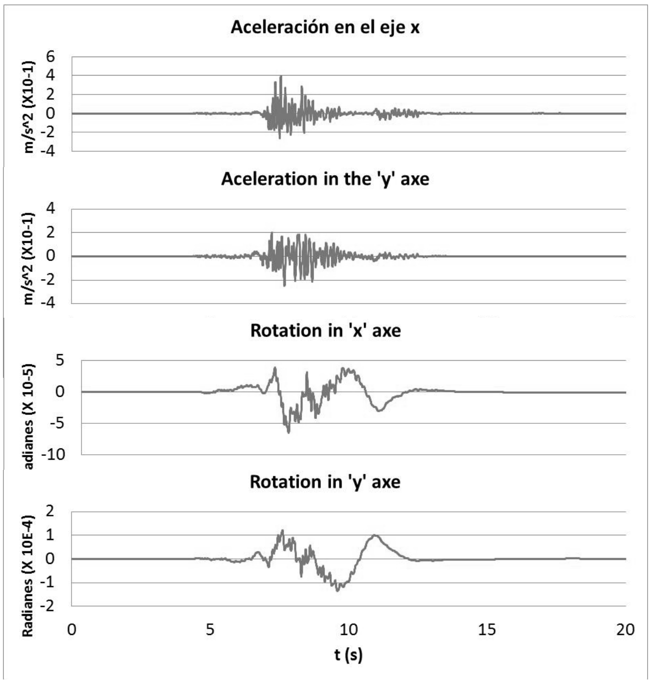

Fig. 2 Time Histories of accelerations an rotations corresponding to the left hand side SF and a focal mechanism of azimut = 222,7º, dip= 32,8º and rake =126.2º

III. Finite Element Model of the Wind Turbine

Of course the simplest dynamical model has only 1 degree of freedom (dof). However, this type of model is not suited to represent adequately the dynamic response of a wind turbine during a seismic event. Much more sophisticated models that include several soil layers represent the opposite extreme leading to prohibitive calculation times. In the latter case 3d continuum elements are used for the soil, shell elements for the tower as well as the blades and concentrated masses to represent heavy equipment located in the nacelle. Fig. 3 presents some views of a wireframe model and a photo.

A good compromise between accuracy and calculation times can be achieved by choosing a Finite Element (FE) model that represents a medium level of sophistication. To this end the soil's stiffness and damping properties are approximated by means of spring and damper elements that are located at the bottom of the footing. Apart from the spring and damper elements additional masses can also be included in order to account for the surrounding soil that accompanies the motion of the footing. The tower, as well as the blades, is modeled using beam elements. If the forces in the blades are not of special interest, rotor, nacelle and the heavy equipment may be modeled by means of concentrated masses at the top of the tower. The resulting FE model permits to study the contribution of the different bending modes to the overall response and allows studying the effects of changes in footing dimensions or soil properties. Therefore this type of model has been used for the simulations.

Fig. 3 Wireframe model and photo of the wind turbine MADE AE-46/1

As already mentioned in previous sections, the upper soil layer is very, very stiff. This should always be remembered when interpreting results presented in the present paper.

The highest excitation frequency is limited to approximately 30 Hz. With this in mind, a convergence study has been performed in order to end up with a suitable FE mesh. The varying diameter and thickness of the tower leads to continuously changing mass and stiffness properties between top and bottom. The used beam elements have a constant cross-section which increases the required number of elements. Finally, a mesh with 45 elements of equal length has been used for the simulations. Table I lists the frequencies and type of the first 8 modes of vibration. The vertical axis is denoted by y.

TABLE I
Vibration Mode Characteristics

Number	Type	Frequency [Hz]	Period [s]
1	Bending x direction	0.7910	1.264
2	Bending z direction	0.7910	1.264
3	Bending x direction	6.7766	0.148
4	Bending z direction	6.7766	0.148
5	Axial transl. y direct.	16.8137	0.059
6	Bending x direction	19.8609	0.050
7	Bending z direction	19.8609	0.050
8	Torsion rot y	26.4675	0.038

Rayleigh damping equivalent to 1 % of critical damping has been used using the frequencies of the first and third modes.

IV. Results

A total of 60 simulations have been carried out, two for each of the 30 sets of time history accelerations: once considering that the ground motion produces only motion on the translational dof at the base, and a second one with additional motion on the rotational dof. For a given seismic input, the results with or without rotational seismic input may be very similar. Comparisons may be established in terms of the maximum value of Von Mises stresses at a given section of the tower. Fig.4 (a) shows this magnitude as a function of the height of the tower considering both kinds of seismic input for a given set of time history accelerations. In this case differences are smaller than 10%. Fig. 4 (b) displays the same plot for a different set. This time differences are much more important, indicating that for this set the base rotations do have a big influence on the response of the tower. The differences on the radiation pattern between both cases as well as resonance effects between vibration frequencies of top soil layer and main structural modes may explain the discrepancies.

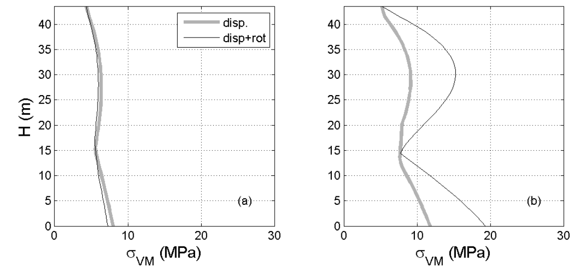

Fig. 4 Comparison of the distribution of maximum Von Mises stress along the tower's height with or without rotational input for records: (a) no.12 and (b) no.18

In Table II the Von Mises stresses at the bottom of the tower of all simulations are resumed.

In order to assess the differences obtained between simulations with or without the rotational seismic input, results from all simulations have been analyzed globally. For each section (height) the maximum value of the Von Mises stress resulting from each simulation has been considered as a realization of a random variable X. It has been assumed that X distributes as a lognormal random variable, and its two parameters have been estimated from the 30 samples available. Fig. 5 shows plots of the probability density functions for both cases at three different heights. At the base (0m) and around 30m both distributions are quite different. However this is not the case at 15m. The reason is that that modes number 3 and 4, which are the ones that are excited significantly by base rotations, have reduced moments at this height.

TABLE II
DETAILED RESULTS COMPARISON

No.	Strike	Dip	Rake	von Mises [Mpa] at the base considering rotational components		Ratio col.5/ col.6
				YES	NO	
1	204.5	23.7	167.9	16.23	10.87	1.493
2	243.2	43.0	158.8	14.08	13.36	1.054
3	277.7	62.3	28.5	15.54	12.24	1.269
4	316.3	79.6	156.7	13.21	13.31	0.992
5	355.0	8.9	152.4	22.56	10.50	2.148
6	33.6	28.2	148.0	17.02	11.52	1.477
7	72.3	47.6	143.6	19.54	11.72	1.667
8	106.8	66.9	139.3	14.96	9.54	1.568
9	145.4	84.1	134.9	12.22	11.27	1.085
10	184.1	13.5	130.5	13.62	9.41	1.446
11	222.7	32.8	126.2	10.71	10.61	1.009
12	261.4	52.1	121.8	7.26	7.99	0.909
13	295.9	71.4	117.4	15.88	13.19	1.204
14	13.1	71.4	121.8	12.05	11.15	1.081
15	51.8	88.7	117.4	10.54	10.52	1.002
16	90.4	18.0	113.1	9.26	8.63	1.072
17	124.9	37.3	108.7	15.73	13.24	1.187
18	163.6	56.6	104.3	19.39	11.81	1.642
19	202.2	76.0	100.0	14.40	8.89	1.620
20	240.9	17.6	95.6	9.09	7.74	1.174
21	279.5	27.3	91.2	17.78	10.33	1.721
22	314.0	36.9	86.9	22.42	13.01	1.723
23	352.7	46.6	82.5	21.01	14.01	1.500
24	31.3	56.3	78.1	8.823	8.63	1.022
25	70.0	64.9	73.8	16.97	10.91	1.555
26	108.6	74.5	69.4	10.47	7.43	1.409
27	143.1	84.2	65.0	27.82	13.26	2.097
28	181.8	3.9	60.7	12.47	8.28	1.503
29	220.4	13.5	56.3	8.56	7.64	1.120
30	259.1	22.1	51.9	22.41	10.20	2.197

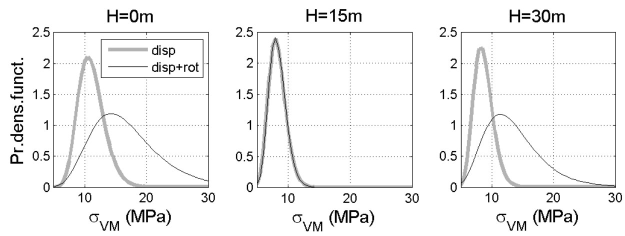

Fig. 5 Comparison of probability density functions of maximum Von Mises stress at sections placed at different heights of the tower

The results indicate that there is a large scatter among results. Some records display important differences while others do not fit this point. It is not clear whether important differences are associated to particular focal mechanism or to particular SF. This question is addressed next.

V. NEW SETS OF SYNTHETIC GROUND MOTIONS

In order to assess the importance of focal mechanisms and SF, three new sets of synthetic ground motions have been generated. In each case, a focal mechanism has been fixed, and the same 30 SF have been applied.

The focal mechanisms are listed in Table III, Sets B and C differ only on their strike angle. Set D has the same characteristic angles as the record of the first set (set A) leading to the highest discrepancies (no.30).

TABLE III
FOCAL MECHANISMS OF THE NEW SETS OF GROUND MOTIONS

Set	Strike	Dip	Rake
B	180	75	175
C	135	75	175
D	259.1	22.1	51.9

VI. RESULTS FOR NEW SETS OF GROUND MOTIONS

For each record of the new sets, again two simulations have been done: one considering the rotational seismic components, and another without them. The importance of the rotational components will be assessed using the following ratio

$$\frac{\max\left(\sigma_{VM,disp+rot}\right)}{\max\left(\sigma_{VM,disp}\right)}. \tag{1}$$

High values of the ratio indicate that rotations are important, while values close to unity indicate the opposite.

Figure 6 displays the cumulative distribution function (CDF) of the ratios for the three sets. Set C has an almost vertical CDF indicating that all the ratios are close to 1. Discrepancies between results with or without rotational components are noticeable for the records in set B, and remarkably important for those in set C.

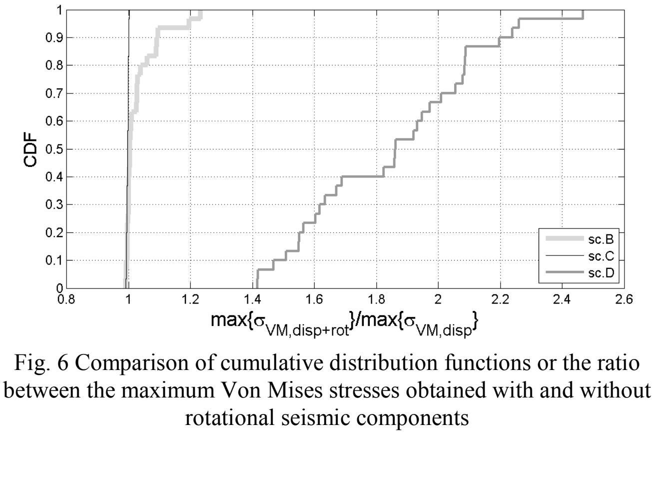

Fig. 6 Comparison of cumulative distribution functions or the ratio between the maximum Von Mises stresses obtained with and without rotational seismic components

VII. CONCLUSION

The results obtained in this study indicate the importance of the rotational components of ground motions on wind turbine response patterns.

The importance of the rotational components is directly related to its magnitude, which is highly dependent on the focal mechanisms. Source time functions have proven to also have an effect on it, but it only arises with suitable focal mechanisms.

ACKNOWLEDGMENT

The work presented in this paper is partly funded Universidad Politécnica de Madrid and by Comunidad Autónoma de Madrid

REFERENCES

[1] Bouchon, M. (1979). "Discrete wave number representation of elastic wave fields in three-space dimensions". J. Geophys. Res. 84, 3609-3614.

[2] Bouchon, M. and Aki, K. (1977). "Discrete wavenumber representation of seismic source wavefield." Bull. Seism. Soc. Am., 67, 259-277.

[3] Corchete V. and M. Chourak, (2011). "Shear-wave velocity structure of the south-eastern part of the Iberian Peninsula from Rayleigh wave analysis". International Journal of Earth Sciences, 100, 1733-1747.

[4] Houston, H. (2007). "Deep Earthquakes," in Treatise on Seismology, ed. H. Kanamori and G. Schubert (Elsevier), 321–350.